Journal of Radiation Research, 2015, 56, 391–396
doi: 10.1093/jrr/rru112 Advance Access Publication 14 January 2015

Application of an ultraminiature thermal neutron monitor for irradiation field study of accelerator-based neutron capture therapy

Masayori ISHIKAWA[1,*], Kenichi TANAKA[2], Satrou ENDO[3] and Masaharu HOSHI[4]

[1]Department of Medical Physics and Engineering, Graduate School of Medicine, Hokkaido University, N-15 W-7 Kita-ku, Sapporo Hokkaido, 060-8638, Japan
[2]Center of Medical Education, Sapporo Medical University, S-1 W-16 Chuo-ku, Sapporo Hokkaido, 060–8543, Japan
[3]Graduate School of Engineering, Hiroshima University, 1–4–1, Kagamiyama, Higashi-Hiroshima, Hiroshima 739–8527, Japan
[4]Research Institute for Radiation Biology and Medicine, Hiroshima University, 1–2–3 Kasumi Minami-ku, Hiroshima Hiroshima 734–8553, Japan
*Corresponding author. Department of Medical Physics and Engineering, Graduate School of Medicine, Hokkaido University, N-15 W-7 Kita-ku, Sapporo Hokkaido, 060–8638, Japan. Tel: +81-11-706-7638; Fax: +81-11-706-7639; Email: masayori@med.hokudai.ac.jp

(Received 8 July 2014; revised 4 September 2014; accepted 5 November 2014)

Phantom experiments to evaluate thermal neutron flux distribution were performed using the Scintillator with Optical Fiber (SOF) detector, which was developed as a thermal neutron monitor during boron neutron capture therapy (BNCT) irradiation. Compared with the gold wire activation method and Monte Carlo N-particle (MCNP) calculations, it was confirmed that the SOF detector is capable of measuring thermal neutron flux as low as 10^5 n/cm^2/s with sufficient accuracy. The SOF detector will be useful for phantom experiments with BNCT neutron fields from low-current accelerator-based neutron sources.

Keywords: neutron capture therapy; SOF detector; thermal neutron monitor

INTRODUCTION

Boron neutron capture therapy (BNCT) is a cancer treatment modality whose therapeutic efficacy relies on both the concentration of boron in the tumor and the thermal neutron flux at tumor sites during irradiation. Boron delivery to the tumor is being addressed by current studies on new boron carriers, while a number of techniques for determining boron concentration, either *in vivo* or *in vitro*, have been proposed in order to perform neutron irradiation at the time when the boron concentration in both the tumor and healthy tissue are at their optimum levels [1]. Most of the neutron fields currently being used for BNCT clinical trials come from research nuclear reactors that have been modified to accommodate BNCT irradiations. The number of these facilities has increased in recent years, but due to the limited number of reactors that can be converted for medical irradiation purposes, there are still very few available BNCT irradiation facilities. One possible solution to this would be accelerator-based neutron sources (ABNS) that can be constructed in hospitals, similar to those used in conventional radiotherapy. At present, there are many accelerator facilities that can potentially be used for neutron production, but most of them are unable to provide the required neutron flux for BNCT due to their low beam currents. Some recently proposed accelerator systems that are to be used mainly for BNCT address this limitation in the beam current [2].

The evaluation of the neutron field in a BNCT irradiation facility is generally performed by measuring the distribution of the thermal neutron flux and the gamma dose rate that is generated in a water phantom. The current method for determining the thermal neutron flux in reactor-based BNCT is by means of gold wire activation. However, this may not be practically applicable to an accelerator-based neutron source because of the low neutron flux, which would require very long exposure of the gold wire to the neutron beam to get meaningful results. Moreover, using the gold wire activation method in an epithermal neutron beam requires the

application of correction factors to account for the relatively large cross-section of neutron absorption in ^{197}Au at ~0.5 eV. Although a relatively precise evaluation of the thermal neutron flux can be obtained from activation of ^{197}Au by using wires with and without a cadmium cover, this method requires that the thermal neutron flux is > 10^6 n/cm^2/s.

Several detectors, including the BF_3 counter, fission chamber, Li-doped semi-conductor detectors (e.g. miniature Si detectors with fission converter U-235, MOSFET paired detectors with one of them covered by a B-10 converter, p-in Si diode response), and self-powered neutron detectors can also be used to measure the thermal neutron flux in BNCT [3–6].

Recently, a Scintillator with Optical Fiber (SOF) detector has been developed for real-time thermal neutron flux monitoring during BNCT irradiation [7, 8]. The SOF detector system can easily perform dose profile measurements in a water phantom. More importantly, because it is equipped with a small probe, it is able to perform measurements in conditions inaccessible for other neutron detectors, (e.g. in very narrow spaces). While theoretical evaluation of BNCT neutron fields may now be carried out with reasonable accuracy via a number of simulation codes, for example the Monte Carlo N-particle (MCNP) transport code [9], actual measurements with these detectors are necessary for verifying the validity of these calculations and for routine checks that need real-time data.

We report here the results of experimental validation of the feasibility of implementing the SOF detector system in accelerator-based BNCT. The SOF detector was benchmarked against the results of MCNP calculation and gold wire–activation measurements.

MATERIALS AND METHODS

SOF detector

Figure 1 is a schematic illustration of the SOF detector, the components of which included a probe with a small amount of plastic scintillator, a plastic optical fiber, a photo-multiplier tube, a charge pre-amplifier, a discriminator and a counter. The plastic scintillator (Bicron BC490, partially polymerized plastic scintillator), which was mixed with a small amount of LiF powder (enriched 95% ^{6}Li), was attached to the tip of the plastic optical fiber (Mitsubishi Rayon MH4002, 1 mm-diameter optical fiber with 2.2 mm-diameter polyethylene shielding). The signal recorded by the SOF detector came from the reaction between the ^{6}Li nuclei and the thermal neutrons that emitted charged particles (alpha and triton), which in turn produced scintillation photons in the plastic scintillator. The photon signals were transmitted through an optical fiber to the Photon Counting Head (Hamamatsu H7155), which was made up of the photo-multiplier tube, charge pre-amplifier and discriminator. These signals were converted into 30 ns-width TTL pulses, which were sent to a personal computer via a USB (Universal Serial Bus) connection for data processing. The SOF detector system was composed of two identical SOF detectors, one with ^{6}LiF and the other without ^{7}LiF (for gamma-ray and fast-neutron compensation).

The calibration for estimating absolute thermal neutron flux was performed using a gold activation method used at the JRR-4 research reactor of the Japanese Atomic Energy Agency (JAEA). The conversion coefficient from the SOF count rate to thermal neutron flux was calibrated as 3.69×10^3

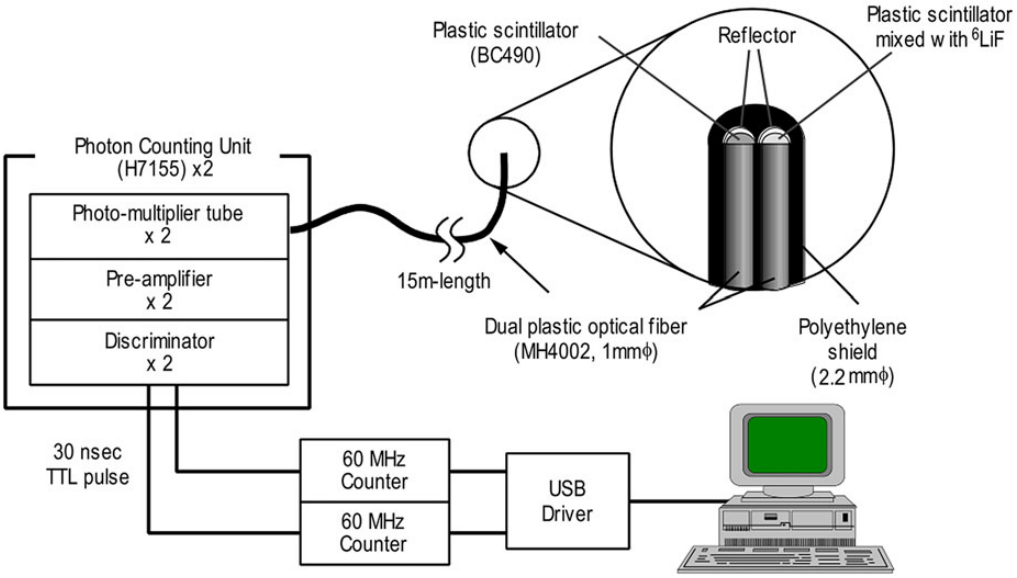

Fig. 1. Schematic diagram of the SOF detector system. This illustrates the components of the SOF detector, including a small plastic scintillator (with and without ^{6}LiF), a plastic optical fiber, a photon counting unit, and a data acquisition system connected to a personal computer via USB.

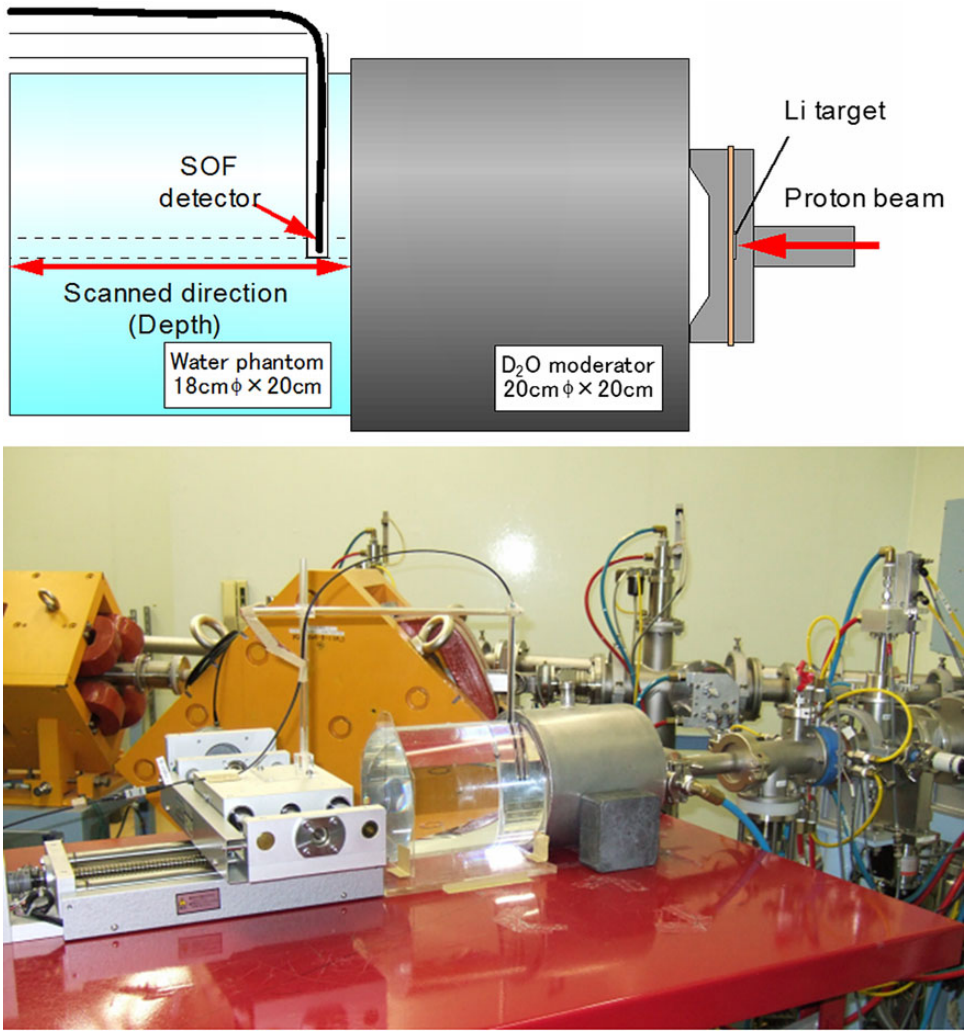

Fig. 2. Experimental setup of phantom experiment. This illustrates the water phantom set behind a D_2O moderator and the SOF detector probe (which is attached to a servomotor-controlled positioning device).

(n/cm^2/s/cps), and we used this conversion coefficient for all experiments.

Accelerator-based neutron source

In this study, neutrons were generated using a Shenkel type single-end accelerator at the Hiroshima University Research Accelerator (HIRRAC), where the maximum accelerator voltage is 3 MV and the maximum beam current of H^+ is 1 mA. A lithium metal target with a diameter of 25 mm and a thickness of 300 µm was used for neutron production via the ^{7}Li(p,n) reaction. While the maximum attainable beam current of HIRRAC is 1 mA, the stable beam current achieved on the day of the experiment was only 50 µA; the HIRRAC beam current is highly dependent on the accelerator condition. With a pure lithium metal target at an accelerator voltage of 2.5 MV, the neutron production rate was ~8.83×10^{11} n/s/mA, which corresponds to a neutron production rate at the lithium target of ~4.42×10^{11} n/s for 50 µA [10].

Thermal neutron flux measurements

One of the indicators of whether a neutron irradiation field will be suitable for BNCT is the thermal neutron flux distribution it generates in a water phantom. Currently, BNCT clinical studies are mainly performed for brain tumors; therefore, the evaluation of the accelerator-produced neutron beam was carried out using a cylindrical water phantom having dimensions similar to a human head under BNCT irradiation. An 18 cmϕ (diameter) × 20 cm (length) cylindrical water phantom constructed from a 3 mm-thick polymethyl methacrylate (PMMA) material was used in the experiment. Figure 2 illustrates the setup for measuring the thermal neutron flux distribution in the water phantom with the SOF detector system. The water phantom was placed behind a 20

cmϕ (diameter) × 20 cm (length) D_2O moderator enclosed in 1-mm-thick stainless steel. The detector probe was set at desired positions in the water phantom using a positioning device controlled by a stepper motor. Thermal neutron flux measurements using the SOF detector were performed at 2.5-mm increments from the inside surface of the phantom up to 20 mm from the outside surface of the phantom, then at 5-mm steps from 20 mm to 50 mm, and at 10-mm increments from 50 mm to 150 mm. Each measurement was performed until the accumulated proton charge was 5×10^{-3} coulomb (i.e. taking ~100 s). The scanned direction was along the beam axis, which was defined as the depth direction in this paper.

The data obtained using the SOF detector were compared with estimated values from gold wire activation measurements. The thermal neutron flux distribution was obtained via the cadmium difference method using 0.7-mm gold wires, with and without cadmium covers (i.e. 0.5-mm thick cadmium tubes). The gold wires were placed along the water phantom central axis from the inside surface of the phantom. The gold wire and cadmium tube (which contained gold wire) were taped onto a 2-mm-thick PMMA plate to fix them as exactly as possible at the central beam axis. The first 15 mm, i.e. 5 to 20 mm from the outside surface of the phantom, were separated into six pieces (2.5 mm each), the next 25 mm (20 to 45 mm) into five pieces (5 mm each), and the last 60 mm (45 to 105 mm) into six pieces (10 mm each). The middle position of each gold wire was plotted as the measured position in later figures.

MCNP calculation

In order to investigate whether the SOF measured data agreed with calculated data, MCNP simulations were carried out using a calculation geometry based on the experimental set-up shown in Fig. 2. The walls around the irradiation room were included in the calculation geometry because the irradiation room was small enough such that scattered neutrons from the walls were expected to have an appreciable contribution to the SOF measured signals. Neutron production via the $^{7}Li(p,n)^{7}Be$ reaction was calculated using the Fortran program LIYIELD.FOR developed by Lee *et al.* [10]. Here, a proton beam having a Gaussian energy distribution ($\sigma = 0.1$ MeV) and an average energy of 2.5 MeV was assumed to be incident on a pure lithium metal target with a diameter of 2.5 mm and a thickness of 300 mm. The thickness of the lithium target was chosen such that it would be sufficient to completely stop an incident 2.5-MeV proton.

The neutron flux at the scintillator layer of the SOF detector probe with ^{6}Li was obtained using the MCNP with more accurate modeling of the $^{6}Li(n,\alpha)^{3}H$ reaction. The same method was used for the calculation of the activation of ^{197}Au. The ENDF-B/VI cross-section library was used in the MCNP calculation.

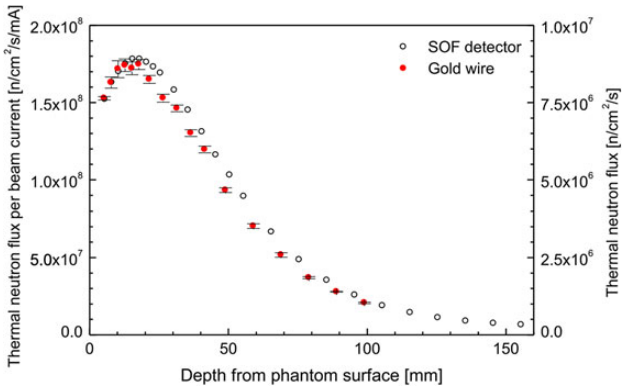

Fig. 3. The evaluated thermal neutron flux from the gold wire and the SOF detector measurements.

RESULTS AND DISCUSSION

Figure 3 illustrates the measured thermal neutron flux using the gold wire activation method and the SOF detector. The vertical axes in this figure correspond to the actual measured thermal neutron flux (right-hand side scale) and the thermal neutron flux normalized per 1 mA of current (left-hand side scale). The data shown for the gold activation measurement are those with cadmium corrections. Error bars for SOF are not indicated in Fig. 3 because the statistical error for the measurements was at most 0.16%. A discrepancy between the data obtained using the gold wire activation method and the SOF detector is observed in Fig. 3. Here, the gold wire activation method appears to have recorded higher fluxes at shallower depths and lower fluxes at deeper parts of the phantom compared with those obtained by the SOF detector. One possible reason for this discrepancy is the self-shielding in the gold wire due to its diameter (0.7 mmϕ , which was chosen in order to gain a higher efficiency of detecting thermal neutrons. On the other hand, self-shielding was not expected in the SOF detector.

In order to clarify this difference in the measured neutron flux, MCNP calculations were performed, the results of which are provided in Fig. 4. Both the SOF-measured data and the flux distribution obtained from the gold wire measurement without cadmium correction agreed fairly well with their respective MCNP-calculated data. On the other hand, the neutron flux distribution derived by MCNP for the gold wire with cadmium correction data was revealed to have overestimated the corresponding experimental neutron flux. Incidentally, MCNP yielded an almost identical result for the simulated data for the SOF detector and the gold wire with cadmium correction.

The discrepancy between the data obtained from MCNP and from the experiment for the cadmium-covered gold wire could be traced to the difference between the calculation geometry and the actual experimental set-up. In the MCNP calculation, the gold wire and cadmium pipe were assumed

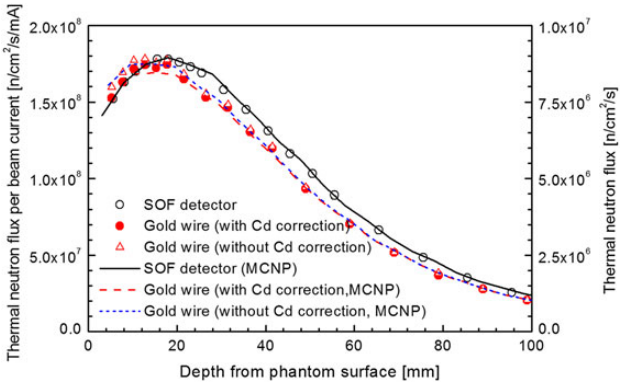

Fig. 4. The MCNP calculated and experimentally measured thermal neutron flux.

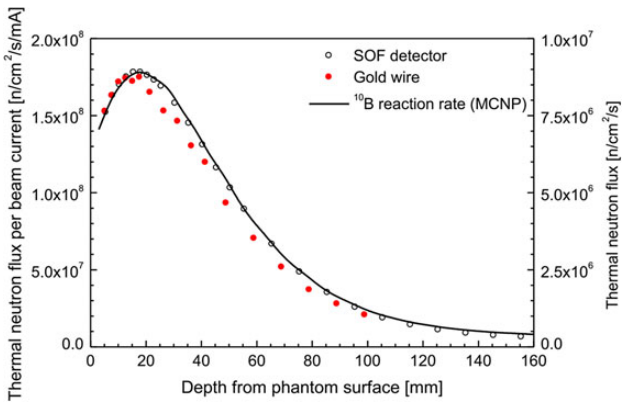

Fig. 5. A comparison of the calculated ^{10}B reaction rate normalized to thermal neutron flux with the experimental data obtained by the SOF detector and gold wire activation method.

to be completely straight (i.e. parallel to the phantom central axis); however, this may not have been exactly the case during the experiment. This could have caused the thermal neutron shielding effect around the cadmium pipe to become bigger, leading to a lower thermal neutron flux for the gold wire placed at deeper sites in the phantom.

The ^{10}B(n,α)^{7}Li reaction rate profile in the phantom is important information for BNCT treatment because this reaction essentially differentiates the dose delivered to healthy or normal tissues and tumors. In Fig. 5, the experimental data obtained by the SOF detector and the gold wire activation method are compared with the calculated ^{10}B reaction rate normalized to the thermal neutron flux. While the SOF detector measurement agreed with the ^{10}B reaction rate, the gold wire activation data under-estimated the ^{10}B reaction rate at central axis depths > 20 mm from the phantom surface. This could have been brought about by the effect of self-shielding, which occurs when relatively thick gold wires (i.e. 0.7 mm in diameter) are used, which would result in a measured thermal neutron flux in deeper parts of a neutron-irradiated medium that is lower the actual value at these depths. With increasing of the depth in water, the ratio of 0.5-eV thermal neutrons to the rest of the neutrons (with lower or higher energies) would change due to moderation of the spectra. The SOF detector can pick up much better moderation of the neutron spectra than Au foil, thus leading to underestimation of Au in a greater depth. It is obvious that the SOF detector is more advanced for BNCT dosimetry, because this detector will provide a response close to B-10.

As demonstrated in Figs 3–5, the SOF detector is capable of accurate thermal neutron flux measurements, even with flux as low as 10^5 n/cm^2/s. For the gold wire method, it will take a few days to measure the thermal neutron flux of 10^6 n/cm^2/s with sufficient accuracy; this is inclusive of the irradiation time and the measurement time. In contrast, it took only 30 min to obtain almost the same data using the SOF detector. This means that the SOF detector system is suitable for phantom experiments to evaluate thermal neutron flux distributions produced by accelerator-based neutron sources, even at low proton beam currents (when low neutron fluxes are expected).

CONCLUSION

In this study, in-phantom thermal neutron flux measurements were performed in order to determine the feasibility of using the SOF detector system for the characterization of neutron irradiation fields from an accelerator-based neutron source for BNCT. Neutron flux distribution measured by the SOF detector was compared with that measured using the gold wire activation method and with estimated data from MCNP in order to demonstrate the accuracy of SOF-measured data.

It has been confirmed that the SOF detector is able to measure thermal neutron flux as low as 10^5 n/cm^2/s with sufficient accuracy, as indicated by good agreement between the experimental and calculated data obtained for the SOF detector. Compared with the gold wire activation method, the SOF detector system offers better flux estimation becuase the activation method requires the use of thick gold wires when measuring neutron flux as low as 10^5 n/cm^2/s, which results in underestimation due to self-shielding.

Finally, this study has demonstrated that the SOF detector system can be implemented in phantom experiments for evaluation of thermal neutron flux distributions generated by accelerator-based neutron sources.

FUNDING

This work was partially supported by Grant-in-Aids for Young Scientists (A) (No. 16689022) by the Ministry of Education, Culture, Sports, Science and Technology.

REFERENCES

1. Nakamura H, Kirihata M. Boron compounds: new candidates for boron carriers in BNCT. In: Sauerwein W, Wittig A, Miss R, Nakagawa Y (eds). *Neutron Capture Therapy – Principles and Applications*. Heidelberg: Springer, 2012, 99–116.
2. Kreiner AJ. Accelerator-based BNCT. In: Sauerwein W, Wittig A, Miss R, Nakagawa Y (eds). *Neutron Capture Therapy – Principles and Applications*. Heidelberg: Springer, 2012, 41–54.
3. Rosenfeld AB, Kaplan GI, Carolan MG *et al*. Simultaneous macro and micro dosimetry with MOSFETs. *IEEE Trans Nucl Sci* 1996;**43**:2693–700.
4. Carolan MG, Rosenfeld AB, Mathur JN *et al*. Characterisation and use of MOSFET gamma dosimeters and silicon PIN diode neutron dosimeters for epithermal neutron beam dosimetry. In: Larsson B, Crawford J, Weinreich R (eds). *Advances in Neutron Capture Therapy*. Amsterdam: Elsevier Science, 1997, 192–7.
5. Kaplan G, Rosenfeld AB, Allen BJ *et al*. Fission converter and MOSFET study of thermal neutron flux distribution in an epithermal neutron therapy beam. *Med Phys* 1999;**26**:1989–1994.
6. Miller ME, Mariani LE, Gonçalves-Carralves ML *et al*. Implantable self-powered detector for online determination of neutron flux in patients during NCT treatment. *Appl Radiat Isot* 2004;**61**:1033–7.
7. Ishikawa M, Ono K, Sakurai Y *et al*. Development of real-time thermal neutron monitor using boron-loaded plastic scintillator with optical fiber for Boron Neutron Capture Therapy. *Appl Radiat Isot* 2004;**61**:775–9.
8. Ishikawa M, Kumada H, Yamamoto K *et al*. Development of a wide-range paired scintillator with optical fiber neutron monitor for BNCT irradiation field study. *Nucl Instr Meth A* 2005;**551**:448–57.
9. Breismeister JF. MCNP a general Monte Carlo N-particle transport code. In: Breismeister JF (ed.) *Technical Report LA-12625-M Version 4B*. Los Alamos: Los Alamos National Laboratory, 1997.
10. Lee CL, Zhou XL, Kudchadker RJ *et al*. A Monte Carlo dosimetry-based evaluation of the ^{7}Li(p,n)^{7}Be reaction near threshold for accelerator boron neutron capture therapy. *Med Phys* 2000;**27**:192–202.